

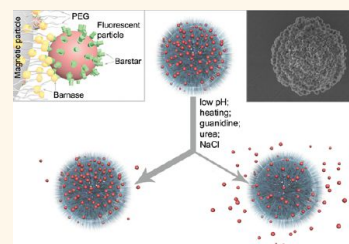
Denaturation-Resistant Bifunctional Colloidal Superstructures Assembled *via* the Proteinaceous Barnase–Barstar Interface

Ulkar F. Aghayeva,^{†,*,#,△} Maxim P. Nikitin,^{†,§,⊥,△} Sergey V. Lukash,[†] and Sergey M. Deyev^{†,||,*}

[†]Shemyakin–Ovchinnikov Institute of Bioorganic Chemistry, Russian Academy of Sciences, 16/10 Miklukho–Maklaya Street, Moscow, Russia 117997,

[‡]School of Biology, Lomonosov Moscow State University, 1 Leninskiye Gory, Moscow, Russia 119234, [§]Prokhorov General Physics Institute, Russian Academy of Sciences, Natural Science Center, 38 Vavilov Street, Moscow, Russia 119991, [⊥]Moscow Institute of Physics and Technology, 9 Institutskii per., Dolgoprudny, Moscow region, Russia 141700, and ^{||}Nizhny Novgorod State Medical Academy, 10/1 Minin and Pozharsky Sq., Nizhny Novgorod, Russia 603005. [△]These authors contributed equally to this work. [#]Present address: Department of Biological Sciences, Columbia University, 1212 Amsterdam Avenue, New York, New York 10027, United States.

ABSTRACT To date, a number of biomolecule-mediated nanoparticle self-assembly systems have been developed that are amenable to controllable disassembly under relatively gentle conditions. However, for some applications such as design of self-assembled multifunctional theragnostic agents, high stability of the assembled structures can be of primary importance. Here, we report extraordinarily high durability of protein-assisted nanoparticle self-assembly systems yielding bifunctional colloidal superstructures resistant to extreme denaturing conditions intolerable for most proteins (*e.g.*, high concentrations of chaotropic agents, high temperature). Among the tested systems (barnase–barstar (BBS), streptavidin–biotin, antibody–antigen, and protein A–immunoglobulin), the BBS is notable due to the combination of its high resistance to severe chemical perturbation and unique advantages offered by genetic engineering of this entirely protein-based system. Comparison of the self-assembly systems shows that whereas in all cases the preassembled structures proved essentially resistant to extreme conditions, the ability of the complementary biomolecular pairs to mediate assembly of the initial biomolecule–particle conjugates differs substantially in these conditions.



KEYWORDS: multifunctional hybrid heterostructures · protein-assisted self-assembly of nanoparticles · colloidal stability · denaturing agents · disassembly in extreme conditions

The principle of molecular recognition is encountered time and again in biological systems and is based on preciseness of structure complementarity of interacting molecules. At the interface of man-made materials and biomolecules, a spectrum of “molecular glues” mediating self-assembly of nanoparticles of various nature has been proposed and investigated in detail.^{1,2} Among them, numerous nanoparticle self-assembly systems have been designed that allow for control of their behavior in terms of assembly–disassembly in different conditions by triggering these transitions with relatively gentle stimuli of various nature. For example, in nucleic acid-based systems, disassembly may be triggered upon temperature denaturation of DNA duplexes holding particles within

the assembly,^{3,4} other examples include disassembly induced by competing oligonucleotides,⁵ lowering of pH (in i-motif DNA-based systems),⁶ and divalent cations of transition metals (*e.g.*, Pb^{2+} (ref 7), Hg^{2+} (ref 8)). Carbohydrate–protein interaction-mediated polymeric particle assemblies can be readily dissociated by addition of Ca^{2+} -chelators (for Ca^{2+} -dependent lectin–carbohydrate interactions)⁹ or low-molecular competing monosaccharides (*e.g.*, glucose, ref 10). Numerous pH-responsive polymer-based nanoparticle self-assembly systems have also been reported.^{11,12} These approaches to achieve controllability of the assemblies using various stimuli have a great potential in the construction of “smart” materials for a number of applications (drug delivery, biosensors,^{7,8,10} *etc.*). Yet in

* Address correspondence to deyeve@ibch.ru.

Received for review June 9, 2012 and accepted January 26, 2013.

Published online January 27, 2013
10.1021/nn302546v

© 2013 American Chemical Society

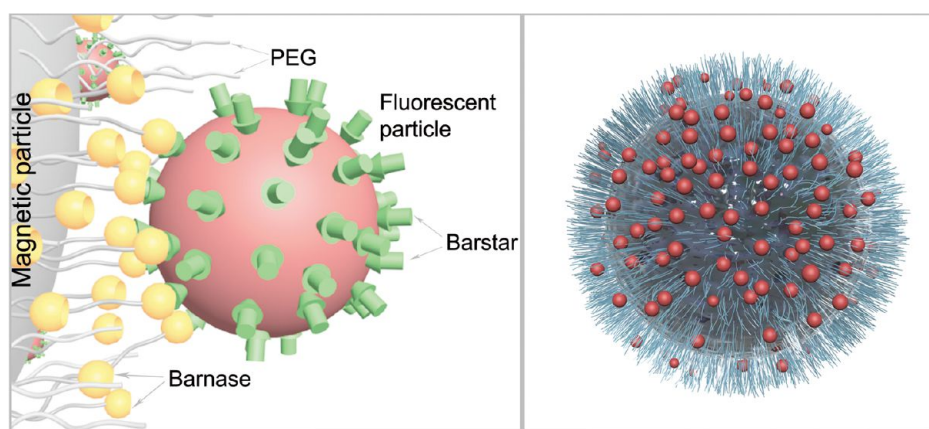


Figure 1. Concept of multipoint contacts between the components of the colloidal assembly. Left: The multiple BBS pairs at the particle interface. Right: General schematic view of an assembled structure. PEG: poly(ethylene glycol).

other situations it is desirable to design materials that would not readily disassemble under appropriate conditions. For example, self-assembled multifunctional theragnostic agents are expected to demonstrate significant stability to ensure retention of all functional modules within a single entity to be able to perform all programmed functions (*e.g.*, imaging, drug delivery, stimulus-responsiveness) with equal efficiency. Here we describe protein-assisted nanoparticle self-assembly systems (namely, those based on barnase–barstar, streptavidin–biotin, antibody–antigen, and protein A–immunoglobulin interactions) that exhibit unexpected robustness in denaturing conditions intolerable for most proteins. Use of proteinaceous “molecular glues” for nanoparticle self-assembly purposes is of interest due to the advantages of introducing new functionalities to the self-assembled structures *via* additional protein modules fused to initial molecules mediating assembly. Among them, we find the barnase–barstar pair particularly noteworthy due to benefits offered by genetic engineering of this entirely protein-based system (see below) and ease of heterologous prokaryotic expression of the proteins in ample amounts.

Barnase and barstar are an excreted ribonuclease and its natural intracellular inhibitor, respectively, both produced by *Bacillus amyloliquefaciens*.¹³ These proteins have been extensively studied with respect to their folding properties¹⁴ and as a model system in the investigation of protein–protein interactions.^{15–18} Remarkably, barnase and barstar are characterized by extremely quick kinetics ($k_{\text{on}} \approx 10^8 \text{ M}^{-1} \cdot \text{s}^{-1}$) and high affinity of binding ($K_{\text{a}} \approx 10^{14} \text{ M}^{-1}$), the latter being second only to that of the streptavidin–biotin system. The proteins are small (12 and 10 kDa, respectively), do not contain intramolecular disulfide bonds, and do not require any cofactors for their folding and function.^{13,18} Barstar inhibits barnase by sterically blocking the active site with an α -helix and adjacent loop segment, forming a 1:1 complex.¹⁹ According to mutagenic experiments¹⁵ and the crystal structure of the barnase–barstar

complex,¹⁹ the binding interface between the proteins primarily consists of polar and charged residues and shows a high degree of electrostatic complementarity.

The barnase–barstar system (BBS) has found applications in bioengineering and design of a number of fusion proteins and supramolecular constructs. To the benefit of barnase and barstar genetic engineering, N- and C-termini of both proteins are not involved in the molecular interface of the proteins within the complex, so they are available for fusions such as those with mini-antibodies,^{20–22} fluorescent proteins,²³ and bacterial toxins,²⁴ which can be used as additional functional modules of the hybrid protein–particle constructions.²² That distinguishes the BBS from the other above-mentioned protein-based self-assembly approaches, which are generally used *per se*.

In this work, we address the question of stability of the BBS-“glued” assemblies subject to destruction. To this end, we test their behavior under severe protein denaturing conditions such as high temperature and low pH as well as high salt and chaotropic agent (urea and guanidinium hydrochloride) concentrations. Experiments show that the obtained constructs possess unusual stability and tolerate conditions far beyond physiological ones. The BBS was also compared to other widely used self-assembly systems mentioned above, in terms of resistance of the preassembled structures to the extreme conditions as well as with respect to their ability to mediate assembly of the initial conjugates involving the components of these systems. Unexpectedly, whereas in the former case the tested systems demonstrate a relatively similar behavior, their performance in the latter differs substantially.

RESULTS AND DISCUSSION

Self-Assembly in Optimal Conditions. Previously, we have shown that the BBS is efficient enough to mediate nanoparticle self-assembly in a “single-point” regime,²⁵

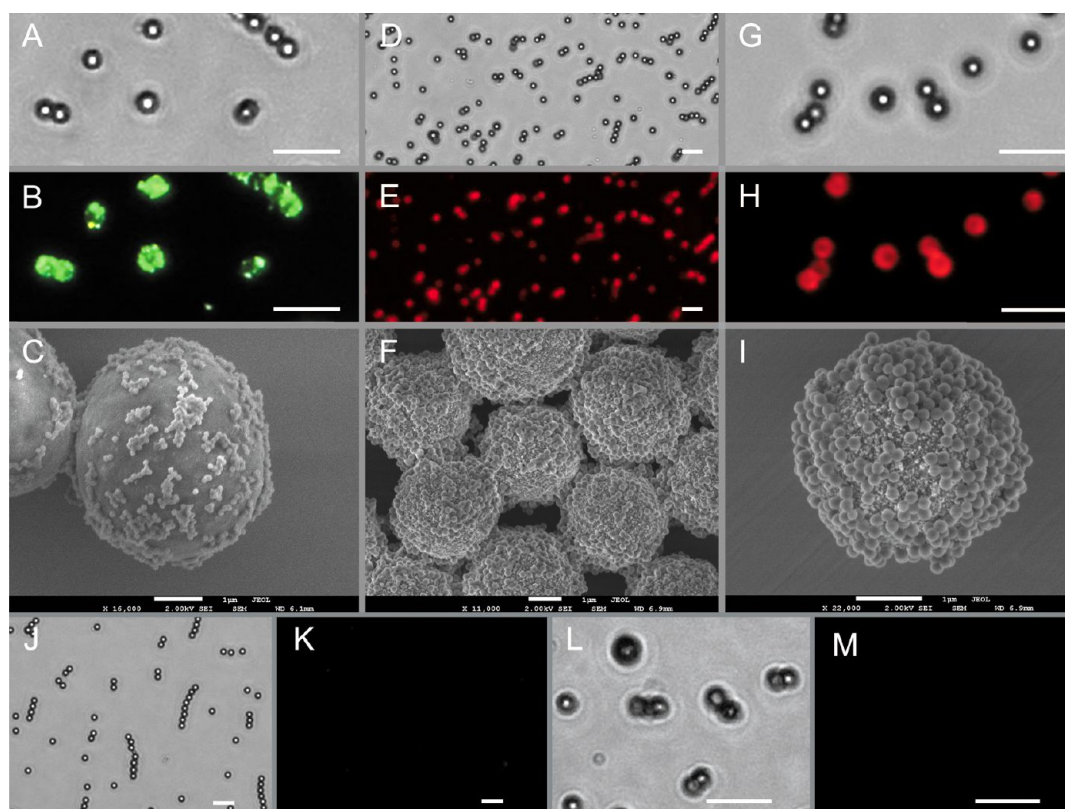


Figure 2. Barnase and barstar are efficient “molecular glues”. Shown are representative optical and SEM images of the BBS-assembled structures. (A) Bright-field image of the large $3.3\ \mu\text{m}$ MPs conjugated with Bn (*via* PEG 10 kDa linkers) and assembled with Bs-coated Yellow 110 nm polystyrene particles. (B) The same assemblies upon excitation of the fluorophore of the Yellow 110 nm particles. (C) SEM image of the same assemblies (a close-up view). (D) Bright-field image of a general view of structures assembled from [MP $3.3\ \mu\text{m}$ –PEG 3 kDa–Bn] and [Purple 200 nm–Bs] conjugates. (E) The same assemblies upon excitation of the fluorophore of the Purple 200 nm particles. (F) SEM image of the assemblies shown in (D) and (E). (G, H) Close-up view of the assemblies shown in (D) and (E), respectively. (I) Close-up SEM image of one of the assemblies from (G) and (H). (J, K) Bright-field and fluorescent images of control conjugates [MP $3.3\ \mu\text{m}$ –PEG 3 kDa–Bn] preblocked with Bs and [Purple 200 nm–Bs] preblocked with Bn and mixed in PBS. Unbound FPs were removed *via* magnetic separation. (L, M) Same as (J, K) but with [Yellow 110 nm–Bs] conjugates as fluorescent modules. Scale bar: $10\ \mu\text{m}$ (A, B, D, E, G, H, J–M) and $1\ \mu\text{m}$ (C, F, I).

wherein the proteins are chemically conjugated directly to the surface of the particles and there are only one or very few barnase–barstar pairs at the contact point. Here, we introduce a modification of the system by using flexible hydrophilic poly(ethylene glycol) derivatives as linkers between the surface of one type of the utilized particles and barnase molecules. Such a modification is believed to allow for increase in the overall colloidal stability of the particles²⁶ as well as for a switch to the “multipoint” binding mode in the resulting assemblies (Figure 1).

In all the experiments described below, $3.3\ \mu\text{m}$ magnetic and 110 or 200 nm fluorescent polystyrene particles were used as functional components of protein-mediated self-assembly. Both types of particles are coated with carboxyl groups, allowing for utilization of robust carbodiimide chemistry for the attachment of amine-containing molecules to the surface of the particles (see Methods). Magnetic particles (MPs) were conjugated with barnase *via* a PEG linker with MW 3 or 10 kDa, whereas fluorescent particles (FPs) were directly conjugated with barstar (Figure 1). We designate the corresponding conjugates as [MP

$3.3\ \mu\text{m}$ –PEG 10 kDa–Bn] and [Fluo $x\ \text{nm}$ –Bs] ([Yellow 110 nm–Bs] or [Purple 200 nm–Bs]). PEGylation was used for one type of particles (larger MPs) only, since, when present on both, it deteriorates the efficiency of self-assembly (ref 27 and data not shown). Moreover, barstar is capable of imparting sufficient colloidal stability to smaller FPs to avoid the necessity of PEG coating.

Purified conjugates of MPs were mixed with fluorescent ones taken in excess in phosphate-buffered saline (PBS) at room temperature to generate structures shown in Figure 2. Here, representative examples of optical and scanning electron microscopy (SEM) images of the resulting assemblies are illustrated. As particles magnetically settled on the surface of the microscope slide prior to visualization, the bright-field and fluorescent images can easily be superimposed. As seen in Figure 2A–C, demonstrating a close-up view of the assemblies formed by mixing MPs conjugated *via* a PEG 10 kDa linker with barnase and barstar-conjugated Yellow 110 nm FPs, fluorescent images clearly indicate the “granularity” of the particle distribution on the surface of MPs and the presence of fluorescing clusters,

which is also confirmed by electron micrographs (Figure 2B, C). Of note, in this case, we used the so-called "Smooth Surface Carboxyl Magnetic Particles" (Spherotech, USA), which resulted in a rather sparse arrangement of FPs and the presence of some "bald" areas on the surface of MPs (see also Figure S1 in the Supporting Information). In contrast, when using nonsmooth Carboxyl Magnetic Particles with an inherently rough and coarse surface and much larger surface area, the resulting assemblies were much more densely covered with FPs (Purple 200 nm; Figure 2D–H). The larger surface area of these particles (compared to the Smooth Surface MPs) likely favored more contacts between the MPs and FPs to be established (see also Figure S2 for assemblies containing 53 nm FPs and nonsmooth MPs). Therefore, for the subsequent experiments, we chose nonsmooth MPs as more efficient building blocks for self-assembly purposes.

Remarkably, the process of self-assembly is robust and rapid: it is sufficient to co-incubate the corresponding conjugates for as little as 5 min to attain *ca.* 50% of the final efficiency of self-assembly in saturating conditions (Figure S3).

It should be noted that optical images represent, though with inferior resolution, the native state of the assembled structures as they appear in aqueous media. In contrast, for SEM experiments, the prerequisite sample preparation procedures include drying, which may lead to artifacts of dehydration of the proteins conjugated to the particles as well as to detachment of small particles from the surface of large MPs in the absence of additional stabilizing agents such as glucose or trehalose.²⁸ Therefore, the obtained SEM micrographs should be treated with caution, as they may give a distorted image of the assemblies. Optical images are more reliable in this regard, since they allow for observation of the resulting assemblies as such, without interference in the spontaneous process of assembly and/or disturbance of the appearance of the structures formed in PBS buffer in optimal conditions. Hence, optical imaging was chosen in subsequent experiments for quantification of the efficiency of self-assembly and the integrity of preassembled structures (see Methods).

As a proof of the high specificity of interactions mediating particle assembly, we performed control experiments with blocking of the barnase- and barstar-conjugated particles with a large molar excess of free barstar or barnase, respectively (Figure 2J–M). In this case, it may be expected that the majority of functionally active surface-conjugated protein molecules (*i.e.*, those capable of binding to the partner protein) will be blocked and excluded from participation in the assembly process. Experiments show that after co-incubation of the blocked magnetic and fluorescent conjugates for the same time and with the same particle ratio as unblocked ones and following

a magnetic separation procedure, no significant fluorescence is observed in the optical microscope at the same exposure. Conjugates of magnetic particles do not exhibit any noticeable inherent fluorescence at even longer exposures. Thus, controls with blocking occur as visual evidence of the high specificity of BBS-driven particle assembly.

Self-Assembly in Extreme Conditions. As mentioned above, barnase and barstar are well known for the remarkably high association constant and inherent individual stability of the proteins. The question that arises from these data regarding purely molecular interactions is whether it is possible to make an extrapolation to interparticle interactions, which are mediated by these molecules. In addition, it is also important to consider interactions between the particles *per se*, involving forces caused by their inherent properties and composition. Could the particle assemblies "glued" with these molecules be more stable than their purely molecular counterparts? To test this, we decided to probe the behavior of the BBS-based particle self-assembly system in conditions that are expected to disrupt specific protein–protein interactions. To this end, we performed two series of experiments aiming at elucidation of the influence of these conditions either (i) on the process of self-assembly itself or (ii) on the integrity of the structures preassembled in optimal conditions. In this section, the first series of experiments is described. In either case, the following conditions were used: (i) exposure to low pH; (ii) incubation in high concentrations of salt (NaCl) or protein denaturants (urea or guanidinium hydrochloride, GdmHCl); (iii) incubation at high temperature (for disassembly experiments only).

Apart from the BBS, we also tested, for comparison, four other common complementary proteinaceous systems, namely, (1) streptavidin·biotin (conjugated to mouse IgG); (2) goat anti-biotin IgG·biotin (conjugated to mouse IgG); (3) rabbit anti-goat IgG·goat anti-biotin IgG; and (4) protein A·rabbit anti-goat IgG. Magnetic particles (nonsmooth 3.3 μm) were conjugated *via* a PEG 3 kDa linker with either barnase, streptavidin, goat anti-biotin IgG, or protein A, while fluorescent ones (Purple 200 nm) were conjugated with either barstar, biotinylated mouse IgG, or rabbit anti-goat IgG. The choice of the functional components of the self-assembly systems was guided by considerations of objectivity of their comparison. Specifically, each of the fluorescent modules, except the one conjugated with barstar, participates in two different systems (see above).

For free proteins barnase and barstar, pH values lower than 4.0–4.5 are known to virtually completely inhibit the formation of the molecular complex.¹³ Surprisingly, even in these conditions (pH 4.0–5.0), we observed the formation of fluorescing MPs, which was as efficient as in PBS. Figure 3 represents an

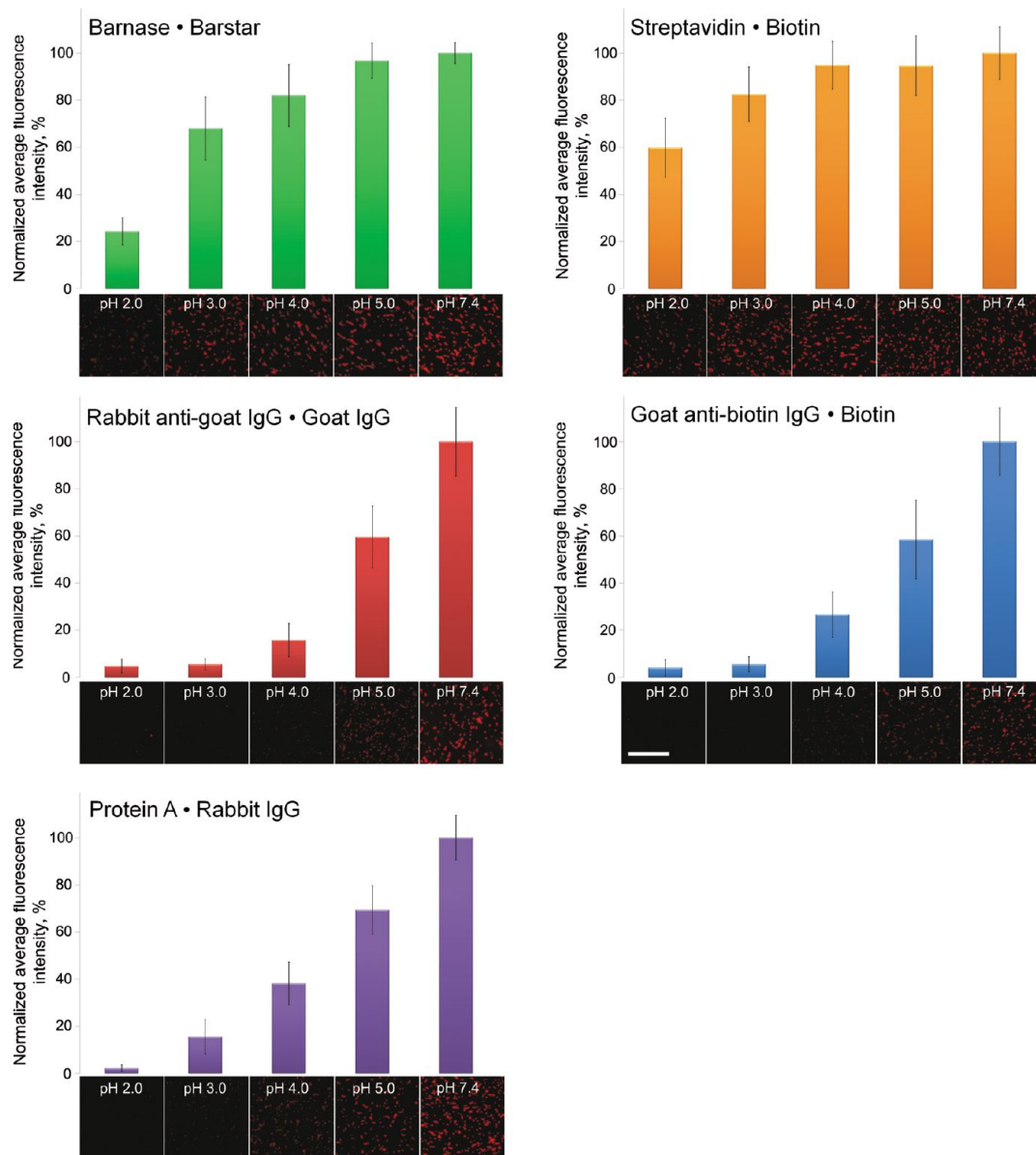


Figure 3. pH-dependence of the efficiency of self-assembly. Scale bar for each photograph is 50 μm .

illustration of the pH-dependence of efficiency of self-assembly for all five systems tested. Each diagram is supplemented with optical photographs demonstrating a gradual decrease of fluorescence of the bifunctional assemblies with lowering of the pH. For systems based on protein–protein interactions (except Bn–Bs), as well as for the [MP 3.3 μm –PEG 3 kDa–Goat anti-biotin IgG]–[Purple 200 nm–Biotinylated mouse IgG] system (GAB–biolGG), pH 5.0 substantially reduces the efficiency of self-assembly, and lower pH values completely inhibit it. In contrast, barnase·barstar and streptavidin·biotin systems proved to be highly resistant to low pH and self-assemble even at pH 3.0, though with decreased productivity. Such behavior of the BBS may be indicative of nonspecific aggregation; therefore, we tested the assembly in the same conditions but in the presence of nonbinding proteins,

to see if that would decrease the contribution of nonspecific interactions (see below).

Urea and guanidinium hydrochloride have been widely used as protein-denaturing agents, yet the detailed mechanism of their action remains controversial. For the denaturing action of urea, two models have been proposed, one based on a direct, favorable interaction between the denaturant and the protein²⁹ and the other based on a modification of the hydrogen-bond structure of water and a consequent weakening of hydrophobic interactions (ref 30 and references therein). According to the former model, urea is believed to directly interact with the peptide backbone of a protein, making hydrogen bonds with the peptide carbonyl groups and displacing water molecules from these sites. In contrast, GdmHCl does not seem to H-bond with the peptide group.³¹ Instead,

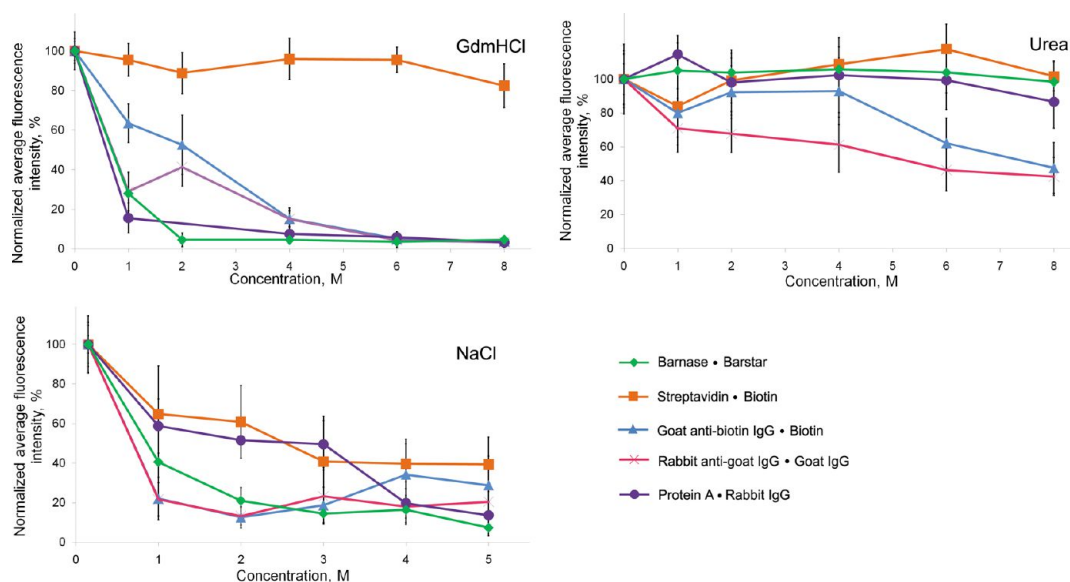


Figure 4. Summary of self-assembly behavior of the five systems under extreme conditions.

due to the high positive electrostatic charge, Gdm^+ could contribute to denaturation of proteins also by direct interactions with negatively charged and solvent-exposed Glu and Asp residues of a protein. Guanidinium is often found to be approximately twice as efficient as urea in denaturing proteins, though this varies with the protein target. In general, the concentration of GdmHCl needed to reach the midpoint of the unfolding transition of a protein is less than that in urea due to the stronger solvation of charged residues and backbone by Gdm^+ than by urea.²⁹

Despite the protein-denaturing effect of urea, with all its concentrations tested (up to 8 M), no noticeable influence on the efficiency of self-assembly has been observed for the BBS: the images of the assemblies formed in its presence are indistinguishable from those generated in PBS. A similar behavior was observed in the case of streptavidin·biotin and protein A·rabbit IgG systems, which also seem to resist the action of urea as well as the BBS does. In contrast, GAb·biolGG and RAG·GAb demonstrate substantially decreased ability to self-assemble in this condition.

In agreement with data concerning their comparative denaturing efficiency, GdmHCl proved to be more efficient in inhibiting the assembly of the initial conjugates than urea; yet even at concentrations as high as 6–8 M, there is still well observable assembly (or aggregation) of the streptavidin/biotin-functionalized particles, whereas all the other systems prove inefficient in these conditions. NaCl at high concentrations (*i.e.*, elevated ionic strength) is the most powerful agent interfering with the process of assembly, which is discernible for the BBS, taking into account the electrostatic nature of interaction between barnase and barstar (see Introduction) (Figure 4). However, all the other systems, including the streptavidin·biotin

system, fail to efficiently self-assemble in NaCl as well. Though the detailed mechanism of molecular interactions in the case of polyclonal antibody-based systems is not clear with respect to contributions of different binding energy components (hydrophobic, electrostatic, *etc.*), all of them are substantially inhibited in this case.

Regarding the streptavidin–biotin system, surprisingly, reasonably high salt concentrations (up to 1 M) are often used to obtain efficient binding of biotin to streptavidin (usually immobilized on a solid support) in various biotechnological applications, suggesting that the interaction is enhanced by the presence of salt ions. The detailed mechanism of participation of salt ions in the streptavidin·biotin interaction remains to be determined.³² Yet, according to the data presented here, 3 M and higher concentrations of NaCl appear to be the only agent capable of substantially inhibiting self-assembly of particles in all the systems, including that based on streptavidin·biotin interaction.

Taking into account the severity of the conditions described above, one could ask whether it is the result of specific self-assembly that is observed or just of plain aggregation of the particles that lost their colloidal stability in these conditions. To address this question, we performed experiments to test the specificity of interactions of the conjugates against other, nonbinding proteins in solution. The rationale behind these experiments is that if the systems used are able to retain the selectivity of interactions (not being blocked with proteins present in the system) and efficiency of self-assembly, then this can be considered as a proof of contribution of authentic biomolecular interactions as mediators of particle self-assembly.

Given the great diversity of proteins in terms of their molecular weight (MW), shape, pI, extent of glycosylation

(if any), hydrophobicity, *etc.*, we expected that the ability of the self-assembly systems used in the present work to assemble in different protein solutions may vary. Thus, we first tested self-assembly in PBS with addition of the following proteins to a final concentration of 1 g/L: (i) bovine serum albumin (BSA), a ~ 67 kDa protein used in numerous biological applications, *e.g.*, as a stabilizer in immunoassays, a blocking agent, and a component of standard buffers; (ii) polyclonal rabbit immunoglobulin G from normal serum; (iii) horseradish peroxidase (HRP), a ~ 44 kDa protein with a 18% carbohydrate content; (iv) thyroglobulin from bovine thyroid, a ~ 670 kDa tetrameric glycoprotein. We also tested self-assembly in 10% human serum diluted with PBS, a cocktail of proteins with various physicochemical properties.

Each of the tested proteins had similar effects on the self-assembly efficiency of the systems (*i.e.*, all systems behaved similarly in the presence of a given protein). Specifically, in BSA, IgG, and HRP solutions self-assembly was on average no less efficient than that in pure PBS (up to 190% of PBS efficiency in different systems), whereas thyroglobulin inhibited assembly by 40–60% (60–40% of that in PBS). As expected, self-assembly in serum showed average efficiency as compared to these two groups of proteins (*i.e.*, about 70% of that in PBS).

Interestingly, BSA has been demonstrated to have a role as a molecular chaperone, that is, a protein able to prevent the misfolding and/or aggregation of other proteins.³³ This stabilization effect of BSA may account for enhancement of specific interactions mediating nanoparticle self-assembly both at physiological and extreme conditions (see below). It is also conceivable that BSA prevents denaturation of the proteins conjugated to the particles, which also adds to the enhancement effect observed.

The described preliminary step allowed us to choose a series of proteins that do not deteriorate self-assembly efficiency. From this series, we selected BSA as the most common reference protein for subsequent experiments involving self-assembly in extreme conditions in the presence of a nonbinding protein. We also performed the same experiments (in the same conditions) varying the concentration of BSA (0.1, 1, 10 g/L) to determine if there is a BSA-concentration dependence of the behavior of the systems. We did not find significant variation in samples prepared in different BSA concentrations in a given condition (all the obtained values were within the limits of experimental error; not shown). Thus, we used intermediate BSA concentration (1 g/L) in subsequent experiments.

Self-assembly experiments were carried out in 8 M GdmHCl, 8 M urea, 5 M NaCl (solutions were prepared by dissolution of the appropriate amounts of the reagents in PBS), and citrate-phosphate buffers with pH 2.0 and 3.0. For each self-assembly system, three samples in each of the mentioned conditions were

tested: (i) in protein-free solutions, (ii) in BSA solutions (BSA was added immediately before the protein–particle conjugates were distributed to the test tubes), and (iii) using conjugates blocked with an excess of partner proteins prior to the self-assembly experiment so that the final concentration of the blocking protein was the same as in BSA solutions (1 g/L). Blocked conjugates were tested for additional corroboration of the specificity of interactions involved in the self-assembly process in extreme conditions.

The obtained data are summarized in Figure 5. It is immediately evident that in the overwhelming majority of experimental points BSA not only has no deteriorative effect on self-assembly efficiency, but, on the contrary, significantly enhances the ability of the systems to assemble in severe denaturing conditions. Notably, whereas NaCl strongly inhibits self-assembly of the systems (including the streptavidin·biotin system) in protein-free solutions, this effect is reversed in BSA solutions: in all cases self-assembly in 5 M NaCl with 1 g/L BSA is much more efficient than that in PBS. At the same time, blocked samples completely lack fluorescent signal, which means that no assembly occurred in these. That is, the unexpected and remarkable effect observed in BSA solutions may be ascribed to enhancement of specific interactions between protein–particle conjugates participating in the self-assembly process, not just to nonspecific aggregation of the particles.

Behavior of the systems in 8 M urea is similar in solutions with and without BSA, within the limits of experimental error, although in most cases BSA also slightly improves self-assembly efficiency in this condition.

In agreement with data presented here, all systems except the streptavidin·biotin system fail to assemble in 8 M GdmHCl, and BSA is not able to improve their performance. The streptavidin·biotin system demonstrates similar self-assembly efficiency in solutions with and without BSA.

Importantly, there are two exceptions of the enhancement effect of BSA in two systems, barnase·barstar and protein A·rabbit IgG, at low pH: in these cases, self-assembly efficiency in BSA solutions is inferior to that in pure buffers. It might be surmised that the observed effect is caused by the fact that self-assembly efficiency in these systems is more susceptible to alterations of the charge profile of the interacting molecules in the pH conditions tested.

Again, in all conditions tested self-assembly of the blocked control particles is not observed, which confirms our assertion regarding predominantly specific interactions between the particles in the course of the self-assembly process.

In summary, for three systems, *i.e.*, streptavidin·biotin, goat anti-biotin IgG·biotin, and rabbit anti-goat IgG·goat IgG, self-assembly in BSA solutions in extreme

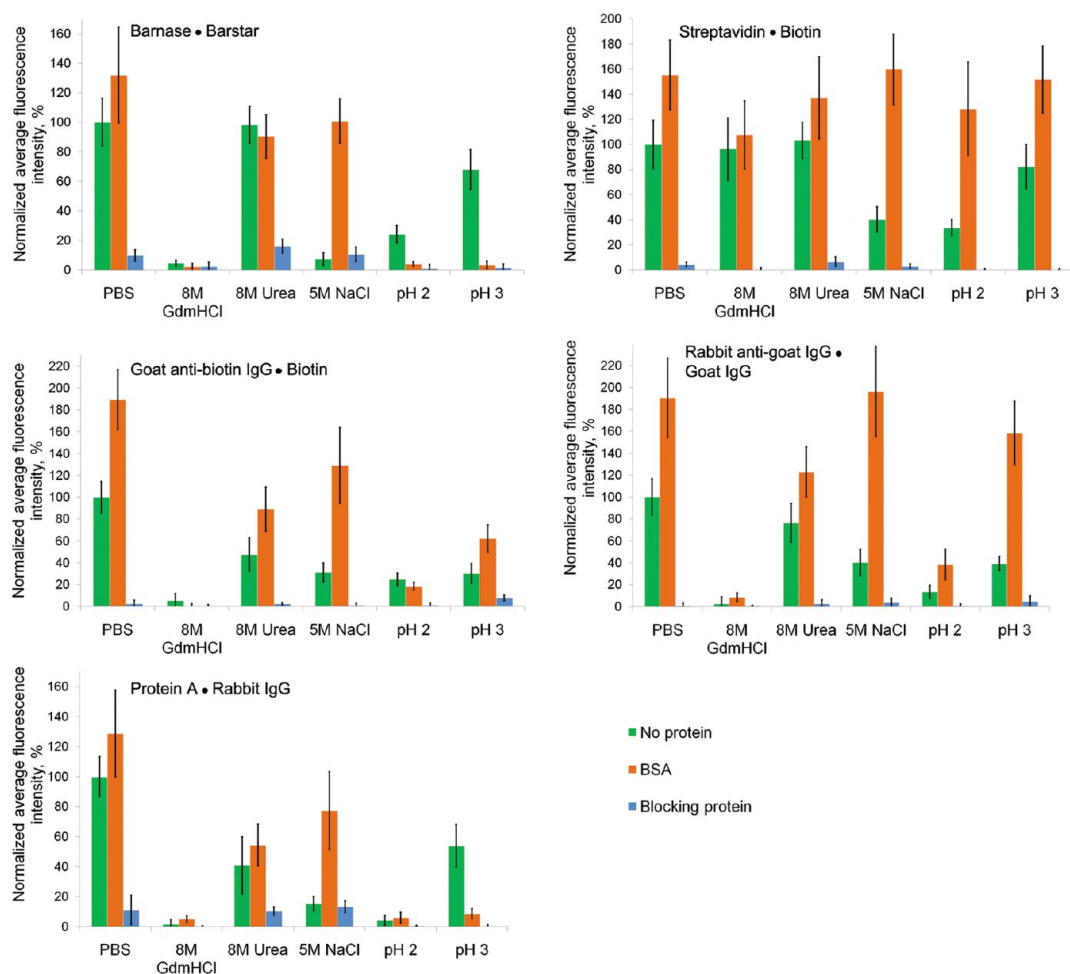


Figure 5. Summary of behavior of the five self-assembly systems in solutions without protein, in 1 g/L BSA solutions, and after blocking with partner protein under denaturing conditions indicated.

conditions appreciably outperforms (or at least is comparable to) that in protein-free solutions. That is also true for the rest of the systems, barnase·barstar and protein A·rabbit IgG, in all conditions except for low pH.

Stability of the Assembled Constructs under Extreme Conditions. In the next experimental setup, the structures preassembled in optimal conditions in PBS were tested in terms of their resistance to increasing concentrations of urea, guanidinium hydrochloride, and NaCl, as described above, heating to up to 80 °C (see Supporting Information, Figure S5), and incubation in acidic buffers with pH ranging from 2.9 to 1.5 for extended periods of time. With respect to the BBS, experiments show that in the case of protein denaturants (urea and GdmHCl) and high ionic strength the influence of these conditions on the integrity of assemblies is less pronounced in comparison with their action on the process of self-assembly itself. That is, once the assemblies are formed, it is much more difficult to disrupt the bonding between them than to prevent their formation from the initial constituents, though the latter also requires extremely harsh conditions. That suggests resemblance to the equilibrium between direct

(forward) and reverse (back) reactions in (bio)chemistry, characterized by the reaction rate constants k_{on} and k_{off} respectively. However, in this case, there is a strong shift toward the direct “reaction” ($k_{on} \gg k_{off}$), making the whole process practically irreversible and thus essentially nonequilibrium.

Among the factors that could contribute to the striking stability of the BBS-assembled structures, in addition to the inherent high bond strength between barnase and barstar, the supposed “multipoint” binding mode of assembly could have played a significant role. A similar idea underlies the concept of avidity in immunology, where the presence of multiple binding sites (two to 10 in antibodies,³⁴ three to 18 and more in collectins and their oligomers³⁵) ensures a very slow rate of dissociation of these receptor molecules from their ligands with multiple epitopes, since for dissociation to occur simultaneous detachment of all ligands is required. An analogous situation may take place in the described self-assembly system as well. Alternatively, the proteins could denature in the conditions tested, but, remaining in close proximity to each other within the complex, they could interact with their unfolded

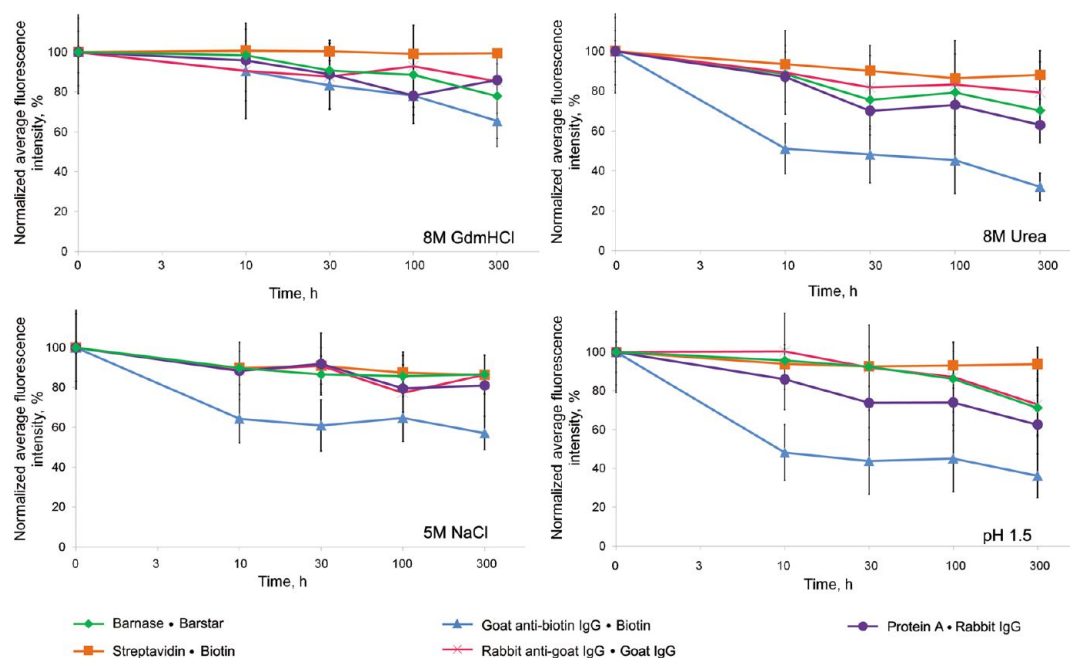


Figure 6. Summary of behavior of the five self-assembly systems upon disassembly of the preassembled structures in protein-denaturing conditions.

hydrophobic regions, thus maintaining the overall appearance of the assembled structures.

Regarding comparison with other self-assembly systems studied (Figure 6), except for the GAb·biolG system, all the rest of the self-assembly systems demonstrate remarkably similar behavior, within the limits of experimental error, with respect to the resistance of preassembled structures to the severe conditions tested. Specifically, the preformed assemblies mostly retain their integrity in protein-denaturing conditions for extended periods of time (up to at least two weeks).

In contrast, their ability to assemble in these harsh conditions (*cf.* Figure 4) differs drastically. The barnase·barstar system demonstrates high stability similar to that of the streptavidin·biotin system, which can be attributed to the robustness of the proteins *per se*. In denaturing conditions that do not completely destabilize the proteins (as GdmHCl and low pH do) the efficiency of self-assembly of the barnase·barstar system is comparable to that in PBS.

Overall, antibody-based systems are more susceptible to denaturing conditions than the BBS and the streptavidin·biotin system in terms of their ability to self-assemble. GdmHCl “permits” assembly of streptavidin/biotin-coated particles only, and that is relatively concentration-independent. Urea-resistant systems include BBS, streptavidin·biotin, and protein A·rabbit IgG pairs. In general, urea proved to be less severe than GdmHCl in inhibiting self-assembly, which correlates with their relative denaturing efficiency toward molecular entities: proteins. NaCl, rather unexpectedly, is a potent inhibitor of self-assembly of all the systems tested in the absence of other proteins in the media.

However, when BSA is added to the solution, the efficiency of self-assembly in high NaCl concentration is comparable to that in PBS for BBS, streptavidin·biotin, and rabbit anti-goat IgG·goat IgG systems. Notably, all conditions demonstrate significantly decreased ability to destruct preassembled structures than to prevent the process of self-assembly from initial constituents.

Comparison of two antibody-based systems, *i.e.*, GAb·biolG and RAG·GAb, allows one to conclude that, apart from effects of denaturation of the proteins, specific interactions within the ligand–receptor pairs are indeed crucial for maintaining the integrity of assemblies. Specifically, it should be noted that in the GAb·biolG system biotin is conjugated to another protein (a mouse antibody in this case), which is also expected to denature under the conditions tested. Thus, both systems contain IgG molecules that are connected by a “receptor–ligand” relation in the case of the RAG·GAb system and a “receptor–ligand carrier” relation in the GAb·biolG system. If the connection between the particles in the assembly were mediated only by nonspecific interactions of the denatured proteins conjugated to their surfaces, then one could anticipate that the GAb·biolG system would not differ much from the RAG·GAb system in its stability and ability to self-assemble in harsh conditions. However, that is not observed: the GAb·biolG system is substantially inferior to the other systems in these qualities, which suggests a nonzero contribution of specific molecular interactions to the observed behavior of the self-assembly systems.

An important finding that follows from the experiments presented here is that hybrid protein–particle self-assembly systems may be much more stable and

resistant to denaturing conditions than the same proteins alone, taken as molecular species. For example, whereas 6 M GdmHCl is routinely used for reversible dissociation of the barnase·barstar complex in affinity chromatography,²¹ the same condition has barely any effect on the integrity of BBS-assembled colloidal structures. However, one should keep in mind that along with specific interactions between self-assembling particles studied herein, van der Waals and other forces in general make a significant contribution to the overall energy of interactions. The question is, what is the relation between the two? Conceivably, that depends not only on individual quantitative contribution of the interaction types but also on the time scale of interactions. We suppose that it is the specific biomolecular interactions that account for initial steps of an assembly formation, allowing van der Waals and other interactions (hydrophobic, electrostatic, etc.) between the particles to strengthen the integrity of the assemblies at later stages, once specific interactions have been established, leading the system to a minimum of potential energy of interactions. This assertion of the “initiating” role of specific interactions is based on the results of control experiments with preblocked conjugates (cf. Figure 2J–M and Figure 5): in this case, van der Waals forces that can potentially be present between the particles cannot assemble them and keep them together, since specific interparticle interactions have been abolished (see Supporting Information for more discussion).

CONCLUSIONS

In this work, we studied the self-assembly of polystyrene micro- and nanoparticles with two functionalities—

magnetic and fluorescent—using proteinaceous “molecular glues”, most notably, the barnase·barstar pair. The obtained assemblies were tested for their resistance to high concentrations of chaotropic agents (urea and GdmHCl) as well as high temperature and low pH conditions causing denaturation of most proteins. In the majority of cases, the structures exhibit unusual stability and maintain apparently unaltered morphologies upon exposure to these conditions for extended periods of time. Comparison of the BBS with other proteinaceous self-assembly systems showed that whereas their resistance to destruction is relatively comparable, the capacity to assemble under harsh conditions differs substantially. Such structures can be used for a number of applications, with examples embracing a broad spectrum including sensing of ecological pollutants in complex media, photonics, and theragnostic approaches in medicine, also making use of multifunctionality offered by the assemblies.

Furthermore, the unexpectedly high stability of the proteinaceous molecular glues described in this work sets one thinking of potential applicability of these self-assembled structures instead of, or along with, covalently linked entities. Using the former, one has access to a great variety of specific (naturally occurring or engineered) “molecular glues” that can be used for the same purposes and with similar efficiency as covalent systems. Moreover, utilization of specific noncovalent interactions adds to the flexibility of the designed assembly systems and imparts higher controllability over the whole process of assembly than in the case of chaotic chemical reactions.

METHODS

Proteins. The following proteins were used for conjugation procedures. Barnase and barstar were produced in *E. coli* and purified as described in our previous work.^{36,37} The purified proteins were stored in the storage buffer (15 mM Tris-HCl, 75 mM NaCl, 1.5 mM EDTA, 32–40% glycerol, pH 8.0) at -20°C . Prior to use, they were either transferred to phosphate-buffered saline using NAP-5 columns (GE Healthcare, USA) or dialyzed against PBS using a Slide-A-Lyzer MINI dialysis device, 7kD MWCO (Thermo Fisher Scientific Inc., USA). Streptavidin (Thermo Fisher Scientific Inc., USA), goat anti-biotin antibody, rabbit anti-goat IgG (H&L), protein A (Rockland Immunochemicals, Inc., USA), polyclonal rabbit immunoglobulin G from normal serum (Jackson ImmunoResearch Laboratories, Inc., USA), bovine serum albumin (Bioclot GmbH, Germany), horseradish peroxidase (BBI Enzymes, USA), thyroglobulin from bovine thyroid (Sigma), and mucin from bovine submaxillary glands (Sigma) were used as obtained. Lyophilized human serum (Vector-Best, Russia) was dissolved in distilled water according to the manufacturer's recommendation and then diluted with PBS to a concentration of 10%.

Conjugation of Magnetic and Fluorescent Particles with PEG Linkers and Proteins. Magnetic polystyrene microparticles (Carboxyl Magnetic 3.3 μm and Smooth Surface Carboxyl Magnetic 3.4 μm polystyrene particles) and fluorescent polystyrene nanoparticles (Carboxyl Fluorescent Yellow 110 nm and Purple 200 nm polystyrene particles) were purchased from Spherotech, USA.

Conjugation of the proteins to the surface of the particles was carried out using the formation of an amide bond between activated carboxyl groups on the particles' surface and amino groups of heterobifunctional PEG molecules (*O*-(2-aminoethyl)-*O'*-(2-carboxyethyl)polyethylene glycol 3000 hydrochloride, Aldrich) and/or proteins. Activation of carboxyl groups was achieved with *N*-(3-dimethylaminopropyl)-*N'*-ethyl carbodiimide (EDC) (using 1:1 to 50:1 EDC to particles mass ratio) in 2-(*N*-morpholino)ethanesulfonic acid buffer, pH 5.0. Typically, 0.5 mg of protein was taken per 1 mg of particles for both barnase and barstar. Both PEG and barnase were conjugated to the magnetic particles using a two-step protocol (*i.e.*, including the removal of excess EDC *via* magnetic separation after activation of the particles and prior to addition of the molecules). Conjugation of barstar to the fluorescent particles was performed as a single-step procedure (*i.e.*, without the EDC washing step). The excess proteins were removed with either a magnetic separator (for magnetic particles) or centrifugation at 16000g for 10–15 min (for fluorescent particles).

Conjugation with other proteins was performed using the above protocol except for quantities of the proteins: 1:10 (or 1:5) protein to particle mass ratio in the case of antibodies, protein A, and streptavidin, according to standard conjugation protocols used for these proteins and recommended by the particle manufacturer.

Self-Assembly of the Conjugates. The prepared conjugates were mixed in different combinations in PBS buffer at room

temperature for 5 min to 24 h (with fluorescent modules taken in excess) with shaking. The assembled structures were isolated from unbound fluorescent particles using a magnetic separation procedure.

Control Experiments. To test the specificity of self-assembly, a series of control experiments was performed: (i) with blocking both the barnase-conjugated and barstar-conjugated particles with an excess of free proteins barstar and barnase, respectively, prior to mixing the conjugates, and (ii) with magnetic particles conjugated (*via* PEG linker) to BSA instead of barnase or barstar. All the self-assembly experiments and their controls were carried out using the same magnetic to fluorescent particle suspension volume ratio.

Instrumentation. The obtained structures were studied using optical and scanning electron microscopy. Optical imaging allowed for immediate visual analysis of the experimental results (particularly, in studying the effects of extreme conditions on self-assembly; see below), whereas SEM was used for pictorial presentation of the appearance of the assemblies. Optical images were acquired with an inverted epifluorescent microscope (Carl Zeiss Axiovert 200) equipped with 10–40× objectives, a 10× eyepiece, and an AxioCam HRC charge-coupled camera. Typically, a drop (1–3 μ L) of the suspension containing the assembled structures was placed on a microscope slide and settled using a strong NdFeB magnet, followed by visualization in bright field and upon excitation of the fluorophore of fluorescent polystyrene particles (at 565/30 nm for Pink 53 nm and Purple 200 nm and 450/490 nm wavelength for Yellow 110 nm polystyrene particles, respectively). The obtained images were processed with AxioVision 4.6 Image software.

Specimens for SEM (scanning electron microscope JEOL JSM-7001F) were applied onto a silicon substrate pretreated with a “piranha” etching solution (a 1:3 (v/v) mixture of 25% hydrogen peroxide, H₂O₂, and 98% sulfuric acid, H₂SO₄) to remove organic impurities followed by rinsing three times in acetone (chemically pure) and then three times in ultrapure 2-propanol. The SEM operated at varying voltages from 2.0 to 10.0 kV with a beam current of 20 pA.

Exposure of the Preassembled Structures to Extreme Conditions. To test their stability, the obtained assemblies were exposed to the following conditions: (i) heating; (ii) incubation at acidic pH (known to disrupt the barnase–barstar complex); incubation in increasing concentrations of (iii) urea in PBS (1 to 8 M), (iv) guanidine hydrochloride in PBS (1 to 8 M), and (v) NaCl (1 to 5 M). Heating was performed in a water bath at 60, 70, 75, and 80 °C for up to 2 h. For testing low pH-resistance of the assemblies, PBS buffer, in which they were stored, was replaced (*via* a magnetic separation procedure) with three to five times as much volume of one of the following buffers: glycine-HCl buffer, pH 2.9, 2.2, or 1.5.

Self-Assembly in Extreme Conditions. Conditions that were the same as above (except heating) were tested for the ability to prevent self-assembly or decrease its efficiency. That is, the initial protein-conjugated magnetic and fluorescent particles (for each of the systems tested) were added to the above solutions and incubated for 1–2 h with shaking and then washed and visualized as described previously. Citrate-phosphate buffers of pH 5.0, 4.0, 3.0, or 2.0 were used instead of glycine-HCl buffers in these experiments.

Quantification of the Data Concerning Behavior of the Self-Assembly Systems under Extreme Conditions. To compare the obtained results with those in optimal conditions (in PBS buffer at room temperature), all the fluorescent images acquired with the same exposure time specific for each condition tested were digitally processed in the following way. Mean fluorescence intensity of the assemblies for each particular case has been assessed by averaging histogram data for 8-bit grayscale versions of the images for 25 particles randomly selected with a circular area with a radius of 14 pixels (given that the total magnification of the microscope was 400×). We understand that this method is somewhat semiquantitative yet sufficient to describe general characteristics of behavior of the assemblies under the above conditions.

Conflict of Interest: The authors declare no competing financial interest.

Acknowledgment. We gratefully acknowledge the Centre for Collective Use of Scientific Equipment, Moscow Institute of Physics & Technology, and, specifically, Evgeny V. Korostylev, for SEM measurements. This work was partially supported by the Russian Foundation for Basic Research (projects nos. 11-04-12091-ofi-m-2011 and 12-04-00757), by the Programs of the Russian Academy of Sciences (Molecular & Cellular Biology and Nanotechnologies & Nanomaterials), and by the Ministry of Education and Science of the Russian Federation (projects nos. 8279, 8843, 16.740.11.0497, 16.523.12.3009, and 16.552.11.7022).

Supporting Information Available: Data regarding comparison of smooth surface and nonsmooth MPs, time dependence of the efficiency of self-assembly, behavior of the studied self-assembly systems in relatively mild denaturing conditions, and thermostability of assemblies. This material is available free of charge *via* the Internet at <http://pubs.acs.org>.

REFERENCES AND NOTES

- Niemeyer, C. M. Nanoparticles, Proteins, and Nucleic Acids: Biotechnology Meets Materials Science. *Angew. Chem., Int. Ed.* **2001**, *40*, 4128–4158.
- Grzelczak, M.; Vermant, J.; Furst, E. M.; Liz-Marzán, L. M. Directed Self-Assembly of Nanoparticles. *ACS Nano* **2010**, *4*, 3591–3605.
- Mirkin, C. A.; Letsinger, R. L.; Mucic, R. C.; Storhoff, J. J. A DNA-Based Method for Rationally Assembling Nanoparticles into Macroscopic Materials. *Nature* **1996**, *382*, 607–609.
- Alivisatos, A. P.; Johnsson, K. P.; Peng, X. G.; Wilson, T. E.; Loweth, C. J.; Bruchez, M. P.; Schultz, P. G. Organization of ‘Nanocrystal Molecules’ Using DNA. *Nature* **1996**, *382*, 609–611.
- Hazarika, P.; Ceyhan, B.; Niemeyer, C. M. Reversible Switching of DNA–Gold Nanoparticle Aggregation. *Angew. Chem.* **2004**, *116*, 6631–6633.
- Wang, W.; Liu, H.; Liu, D.; Xu, Y.; Yang, Y.; Zhou, D. Use of the Interparticle i-Motif for the Controlled Assembly of Gold Nanoparticles. *Langmuir* **2007**, *23*, 11956–11959.
- Liu, J.; Lu, Y. Stimuli-Responsive Disassembly of Nanoparticle Aggregates for Light-Up Colorimetric Sensing. *J. Am. Chem. Soc.* **2005**, *127*, 12677–12683.
- Liu, L.; Zhang, D.; Zheng, X.; Wang, Z.; Zhu, D. Thymine Protected Gold Nanoparticles: Assembly and Disassembly of Gold Nanoparticles in the Presence of Hg²⁺. *J. Nanosci. Nanotechnol.* **2009**, *9*, 3975–3981.
- Hiddessen, A. L.; Rodgers, S. D.; Weitz, D. A.; Hammer, D. A. Assembly of Binary Colloidal Structures *via* Specific Biological Adhesion. *Langmuir* **2000**, *16*, 9744–9753.
- Aslan, K.; Zhang, J.; Lakowicz, J. R.; Chris, D.; Geddes, S. Saccharide Sensing Using Gold and Silver Nanoparticles—A Review. *J. Fluoresc.* **2004**, *14*, 391–400.
- Ding, Y.; Xia, X.; Zhai, H. Reversible Assembly and Disassembly of Gold Nanoparticles Directed by a Zwitterionic Polymer. *Chem.—Eur. J.* **2007**, *13*, 4197–4202.
- Tan, J.; Liu, R.; Wang, W.; Liu, W.; Tian, Y.; Wu, M.; Huang, Y. Controllable Aggregation and Reversible pH Sensitivity of AuNPs Regulated by Carboxymethyl Cellulose. *Langmuir* **2010**, *26*, 2093–2098.
- Hartley, R. W. Barnase–Barstar Interaction. In *Methods of Enzymology*; Elsevier Academic Press Inc.: San Diego, CA, 2001; Vol. 341, p 599.
- Fersht, A. R. Protein Folding and Stability—the Pathway of Folding of Barnase. *FEBS Lett.* **1993**, *325*, 5–16.
- Schreiber, G.; Fersht, A. R. Energetics of Protein–Protein Interactions: Analysis of the Barnase–Barstar Interface by Single Mutations and Double Mutant Cycles. *J. Mol. Biol.* **1995**, *248*, 478–486.
- Timofeev, V. P.; Novikov, V. V.; Tkachev, Ya. V.; Balandin, T. G.; Makarov, A. A.; Deyev, S. M. Spin Label Method Reveals Barnase–Barstar Interaction: a Temperature and Viscosity Dependence Approach. *J. Biomol. Struct. Dynam.* **2008**, *25*, 525–534.
- Sekatskii, S. K.; Favre, M.; Dietler, G.; Mikhailov, A. G.; Klinov, D. V.; Lukash, S. V.; Deyev, S. M. Force Spectroscopy of Barnase–Barstar Single Molecule Interaction. *J. Mol. Recognit.* **2010**, *23*, 583–588.

18. Schreiber, G. Methods for Studying the Interaction of Barnase with Its Inhibitor Barstar. In *Methods in Molecular Biology*; Shein, C. H., Ed.; Humana Press: New York, 2001; Vol. 160, p 213.
19. Buckle, A. M.; Schreiber, G.; Fersht, A. R. Protein-Protein Recognition: Crystal Structural Analysis of a Barnase-Barstar Complex at 2.0-Å Resolution. *Biochemistry* **1994**, *33*, 8878–8889.
20. Deyev, S. M.; Waibel, R.; Lebedenko, E. N.; Schubiger, A. P.; Plückthun, A. Design of Multivalent Complexes Using the Barnase*Barstar Module. *Nat. Biotechnol.* **2003**, *21*, 1486–1492.
21. Semenyuk, E. G.; Stremovskiy, O. A.; Edelweiss, E. F.; Shirshikova, O. V.; Balandin, T. G.; Buryanov, Ya. I.; Deyev, S. M. Expression of Single-Chain Antibody-Barstar Fusion in Plants. *Biochimie* **2007**, *89*, 31–38.
22. Deyev, S. M.; Lebedenko, E. N. Multivalency: The Hallmark of Antibodies Used for Optimization of Tumor Targeting by Design. *BioEssays* **2008**, *30*, 904–918.
23. Lebedenko, E. N.; Balandin, T. G.; Edelweiss, E. F.; Georgiev, O.; Moiseeva, E. S.; Petrov, R. V.; Deyev, S. M. Visualization of Cancer Cells by Means of the Fluorescent EGFP-Barnase Protein. *Dokl. Biochem. Biophys.* **2007**, *414*, 120–123.
24. Prior, T. I.; FitzGerald, D. J.; Pastan, I. Barnase Toxin: A New Chimeric Toxin Composed of Pseudomonas Exotoxin A and Barnase. *Cell* **1991**, *64*, 1017–1023.
25. Nikitin, M. P.; Zdobnova, T. A.; Lukash, S. V.; Stremovskiy, O. A.; Deyev, S. M. Protein-Assisted Self-Assembly of Multifunctional Nanoparticles. *Proc. Natl. Acad. Sci. U. S. A.* **2010**, *107*, 5827–5832.
26. Elbert, D. L.; Hubbell, J. A. Surface Treatments of Polymers for Biocompatibility. *Ann. Rev. Mat. Sci.* **1996**, *26*, 365–394.
27. Harris, T. J.; von Maltzahn, G.; Derfus, A. M.; Ruoslahti, E.; Bhatia, S. N. Proteolytic Actuation of Nanoparticle Self-Assembly. *Angew. Chem., Int. Ed.* **2006**, *45*, 3161–3165.
28. Harris, J. R. Negative Staining of Thinly Spread Biological Particulates. In *Methods in Molecular Biology*; Hajibagheri, N., Ed.; Humana Press Inc.: Totowa, NJ, 1999, pp 13–30.
29. O'Brien, E. P.; Dima, R. I.; Brooks, B.; Thirumalai, D. Interactions between Hydrophobic and Ionic Solutes in Aqueous Guanidinium Chloride and Urea Solutions: Lessons for Protein Denaturation Mechanism. *J. Am. Chem. Soc.* **2007**, *129*, 7346–7353.
30. Camilloni, C.; Guerini Rocco, A.; Eberini, I.; Gianazza, E.; Broglia, R. A.; Tiana, G. Urea and Guanidinium Chloride Denature Protein L in Different Ways in Molecular Dynamics Simulations. *Biophys. J.* **2008**, *94*, 4654–4661.
31. Lim, W. K.; Rösger, J.; Englander, S. W. Urea, but Not Guanidinium, Destabilizes Proteins by Forming Hydrogen Bonds to the Peptide Group. *Proc. Natl. Acad. Sci. U. S. A.* **2009**, *106*, 2595–2600.
32. Holmberg, A.; Blomstergren, A.; Nord, O.; Lukacs, M.; Lundeberg, J.; Uhlén, M. The Biotin-Streptavidin Interaction Can Be Reversibly Broken Using Water at Elevated Temperatures. *Electrophoresis* **2005**, *26*, 501–510.
33. Finn, T. E.; Nunez, A. C.; Sunde, M.; Easterbrook-Smith, S. B. Serum Albumin Prevents Protein Aggregation and Amyloid Formation and Retains Chaperone-like Activity in the Presence of Physiological Ligands. *J. Biol. Chem.* **2012**, *287*, 21530–21540.
34. Janeway, C. A.; Travers, P. *Immunobiology. The Immune System in Health and Disease*, 7th ed.; Current Biology Publications/Garland Sciences: New York, 2007; Chapter 3.
35. Håkansson, K.; Reid, K. B.M. Collectin Structure: A Review. *Protein Sci.* **2000**, *9*, 1607–1617.
36. Edelweiss, E.; Balandin, T. G.; Ivanova, J. L.; Lutsenko, G. V.; Leonova, O. G.; Popenko, V. I.; Sapozhnikov, A. M.; Deyev, S. M. Barnase as a New Therapeutic Agent Triggering Apoptosis in Human Cancer Cells. *PLoS ONE* **2008**, *3*, e2434.
37. Hartley, R. W.; Rogerson, D. L., Jr. Barnase. *Prep. Biochem.* **1972**, *2*, 229–242.